Applied Mechanics and Materials
ISSN: 1662-7482, Vol. 865, pp 434-441
doi:10.4028/www.scientific.net/AMM.865.434

Submitted: 2016-11-20
Revised: 2017-02-07
Accepted: 2017-02-22
Online: 2017-06-02

Damping Force and Energy Regeneration Characteristics of the Regenerative Pendulum Vibration Absorber

Skriptyan Noor Hidayatullah Syuhri[1, a*] and Nasrul Ilminnafik[1, b]

[1]Department of Mechanical Engineering, University of Jember, Jember – 68121, Indonesia

[a,*]skriptyan.syuhri@unej.ac.id, [b]nasrul.teknik@unej.ac.id

Keywords: Pendulum, Vibration absorber, Energy regeneration, Damping force.

Abstract. This paper presents the characteristics of damping force and energy regeneration of a pendulum. The damping force analysis includes force-displacement and force velocity loops when the pendulum, attached in a cart, is subjected with sinusoidal displacement input. The energy regeneration analysis includes the voltage, the current and the power generated by a generator. The main objectives of this paper are to obtain the mathematical models and to characterize both force and energy regeneration based on the inputs. The results show that the amplitudes and the frequencies at low level are most likely basic damper behavior. Moreover, the energy regeneration increases as well as the amplitude and the frequency.

Introduction

Pendulum as a vibration absorber has been of interest of many researchers. In the development of the pendulum, it can be classified as passive, semi-active and active due to the ability to suppress vibrations. Nowadays the pendulum is not only to minimize vibrations but also to harvest energy [1-6]. The vibration energy is converted by a mechanism to produce useful energy such as electric power.

Based on the energy conversion, energy harvesting on the pendulum can be derived and classified into three main categories such as piezoelectric, linear generator and rotary generator [7]. Reported on [8], the rotary generator has several advantages compared with the linear generator and the piezoelectric such as an issue regarding its reliability and its ability to produce sufficient damping force. To optimize the rotary generator performance, it must rotate in unidirectional motion, as suggested by [9].

Considering the advantage of unidirectional motion converter as developed by [10], the aims of this paper are to derive mathematical models of the pendulum using motion rectifier and to study the characteristics of damping force and energy regeneration produced by its systems. The main contributions are to design the systems, to propose some mathematical models and to get the feasibility of the systems as vibration absorber and energy regenerator.

Design and Modeling

Proposed Design. The proposed design of the Regenerative Pendulum Vibration Absorber (RPVA) is depicted in Fig. 1(a). Overall, it consists of bevel gears, clutches, a planetary gear, a generator, a pendulum and an energy regeneration unit. The construction of bevel gears is such a rectifier motion. Gear 1 (8) can only rotate in the counterclockwise (CCW) and Gear 2 (3) can only rotate in the clockwise (CW). Therefore, Gear 3 (5) can definitely rotate unidirectional motion even though the pendulum (5) rotates bidirectional motion. This configuration is caused by clutch (2) and (4). Therefore, Gear 1 (8) and Gear 2 (3) will always have opposite direction.

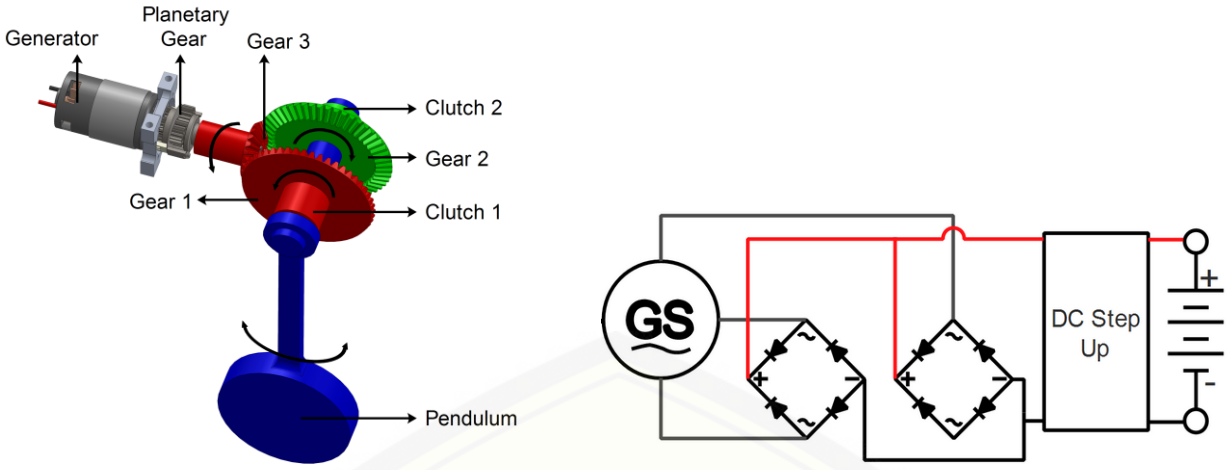

(a) (b)

Fig. 1. System layout of (a) the RPVA, and (b) an energy regeneration unit

The physical device of an energy regeneration unit is shown in Fig. 1(b). It consists of a 3-phase rectifier, a DC step up and a 12V battery. The 3-phase AC generator is rectified into DC current using the 3-phase rectifier arranged as shown in Fig. 1(b). DC step up is used to boost up the DC voltage, so the output voltage is sufficient to charge the 12V battery.

Modeling of Energy Regeneration Unit. Considering the physical device of the energy regeneration unit as shown in Fig. 1(b), the 3-phase AC generator, the 3-phase rectifier and the DC step up voltage can be classified as a set of DC generator. In the other hand, the DC step up device and the battery can be considered as a set of external resistance. Then the diagram analysis of the energy regeneration unit can be simplified as shown in Fig. 2.

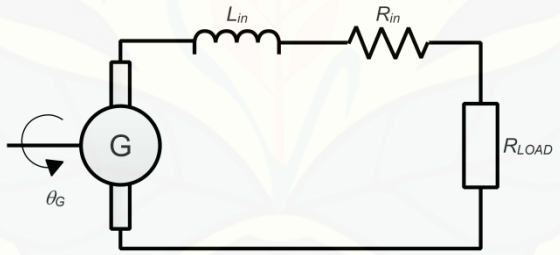

Fig. 2 Simplified diagram of the energy regeneration unit

Based on the Kirchhoff's voltage law, the back electromotive force (*EMF*) and the electric torque, the following relations can be obtained as follows,

$$\begin{cases} E_m - L\dfrac{di}{dt} - (R_{in} + R_{LOAD})i = 0 \\ E_m = k_m\dot{\theta}_G \\ T_e = k_t i \end{cases} \tag{1}$$

where, L and i are the generator internal inductance and the electric current, respectively. R_{in} and R_{LOAD} are the internal generator resistance and the external resistance, respectively. T_e and k_t represent the electrically induced torque and torque constant, respectively. E_m, k_m and $\dot{\theta}_G$ are the mechanically induced voltage, the generator EMF constant and the generator angular velocity, respectively.

In addition, the generator internal inductance is small and can be neglected. Hence, Eq. (1) can be reformed to obtain the electric current as follows,

$$i = \frac{k_m}{R_{in} + R_{LOAD}}\dot{\theta}_G \tag{2}$$

Modeling of the RPVA. The dynamic modeling of the RPVA is illustrated in Fig. 3. The systems are attached to a sliding cart. When the cart is subjected by force in the left direction, the pendulum will rotate in the CCW direction as shown in Fig. 3(a), the motion of the pendulum is transmitted into Gear 1 by shaft. In this motion, clutch 1 engages and clutch 2 disengages. These configurations make Gear 2 free to rotate. On the contrary, when the cart moves on the right direction, the pendulum will rotate in CW direction as shown in Fig. 3(b). It means that clutch 1 disengages and clutch 2 engages. Therefore, force in the pendulum is transmitted into Gear 2 and Gear 1 is free to rotate.

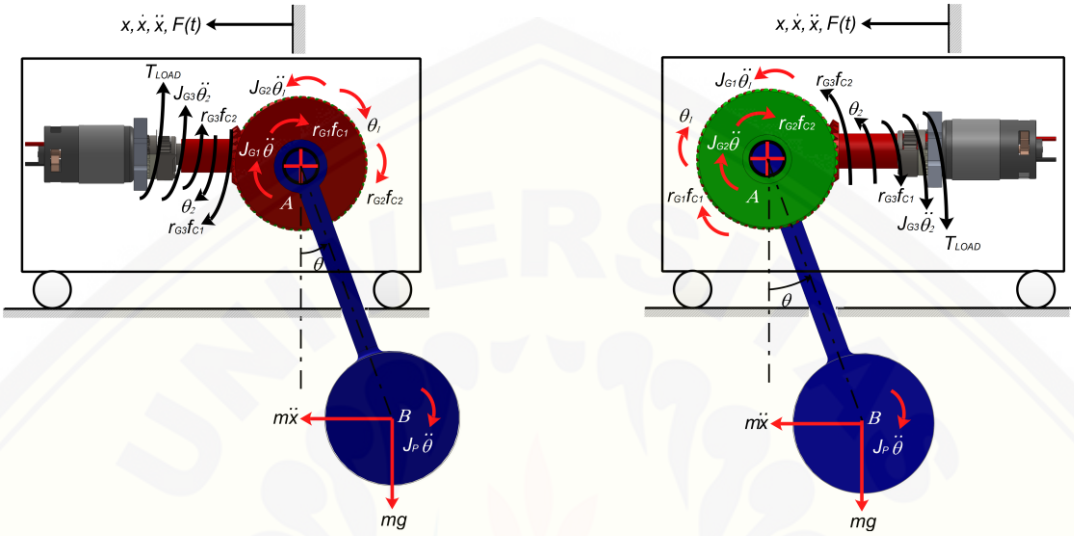

(a) (b)

Fig. 3 Dynamic model of the RPVA (a) Front view, and (b) Back view

Considering the pendulum's motions, CW and CCW are determined as negative and positive direction, respectively. Hence, the equations of motions both in Fig. 3(a) and in Fig. 3(b) can be written based on the D'Alembert's law as follows,

$$\left.\begin{aligned} m\ddot{x} + F(t) &= 0 \\ (J_P + J_{G1})\ddot{\theta} + m\ddot{x}L\cos\theta + r_{G1}f_{C1} + mgL\sin\theta &= 0 \\ J_{G2}\ddot{\theta}_2 - r_{G2}f_{C2} &= 0 \\ J_{G3}\ddot{\theta}_3 + T_{LOAD} + r_{G3}f_{C2} - r_{G3}f_{C1} &= 0 \end{aligned}\right\} \theta \geq 0$$

$$\left.\begin{aligned} m\ddot{x} + F(t) &= 0 \\ (J_P + J_{G2})\ddot{\theta} + m\ddot{x}L\cos\theta + r_{G2}f_{C2} + mgL\sin\theta &= 0 \\ J_{G1}\ddot{\theta}_1 - r_{G1}f_{C1} &= 0 \\ J_{G3}\ddot{\theta}_3 + T_{LOAD} + r_{G3}f_{C1} - r_{G3}f_{C2} &= 0 \end{aligned}\right\} \theta < 0 \qquad (3)$$

where, m and g are the pendulum mass and the gravity acceleration, respectively. L and F define the length of A point to B point and the external force on the cart, respectively. J_P, J_{G1}, J_{G2} and J_{G3} represent the moment of inertia of Gear 1, Gear 2 and Gear 3, respectively. θ, θ_1, θ_2 and θ_3 are the rotation angle of pendulum, Gear 1, Gear 2 and Gear 3, respectively. r_{G1}, r_{G2}, and r_{G3} signify the radius of Gear 1, Gear 2 and Gear 3, respectively. f_{C1} and f_{C2} are the contact force in 1 and 2. T_{LOAD} is defined as torque needed to rotate the planetary gear and the generator.

To obtain the moment of inertia in the planetary gear, first the system and notation are sketched in the Fig. 4(a). The carrier works as an input of rotation. Therefore the angular velocity of the carrier ($\dot{\theta}_c$) is equal to the Gear 3 ($\dot{\theta}_3$). The relations of angular velocity in each gear can be linked by equations as follows,

$$\begin{cases} \dot{\theta}_p = \left(1 - \dfrac{r_r}{r_p}\right)\dot{\theta}_c \\ \dot{\theta}_s = \left(1 + \dfrac{r_r}{r_s}\right)\dot{\theta}_c \end{cases} \tag{4}$$

where, $\dot{\theta}_c$, $\dot{\theta}_p$ and $\dot{\theta}_s$ are the angular velocity of the carrier, the planet gear and the sun gear, respectively. r_c, r_p and r_s are the radius of the carrier, the planet gear and the sun gear, respectively.

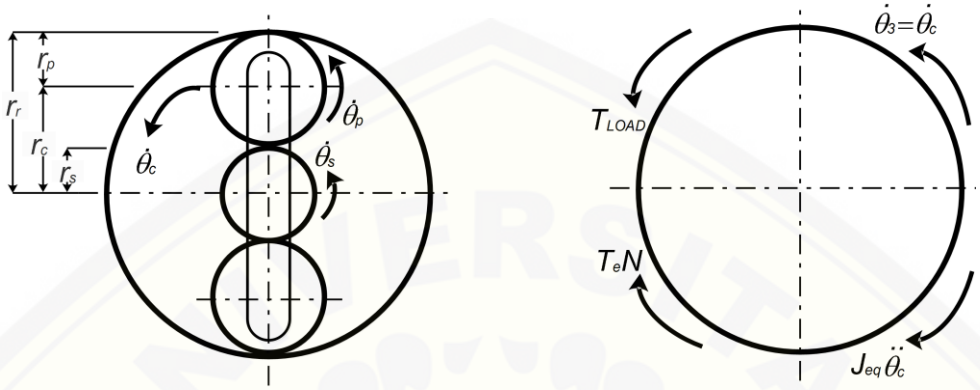

(a) (b)

Fig. 4 (a) Configuration model of the planetary gear; and (b) Free body diagram of the planetary gear and the generator

Taking advantage of the kinetic energy produced by the internal gear system, the equivalent moment of inertia can be calculated with reference to the carrier as follows,

$$J_{eq} = J_s\left(\frac{\dot{\theta}_s}{\dot{\theta}_c}\right)^2 + \left(J_c + nm_p r_c^2\right) + nJ_{pl}\left(\frac{\dot{\theta}_p}{\dot{\theta}_c}\right)^2 \tag{5}$$

where, J_{eq} represents the equivalent moment of inertia of the planetary gear. n and m_p are the number of the planet gear and the planet gear mass, respectively. J_c, J_{pl} and J_s are the moment of inertia of the carrier, the planet gear and the sun gear.

Regarding the equivalent model of the planetary gear and the energy regeneration unit, the free body diagram of the models is illustrated in Fig. 5b. Here the angular velocity of the sun gear ($\dot{\theta}_s$), determined as an output of the gear, is equal to the generator ($\dot{\theta}_G$). Hence, the following mathematical models of Fig. 4(b) can be expressed as follows,

$$J_{eq}\ddot{\theta}_3 + T_eN = T_{LOAD} \tag{6}$$

where, N designates as the gear ratio of the carrier (r_c) and the sun gear (r_s).

Now there are 6 governing equations with several unknown parameters. By eliminating f_{C1}, f_{C2}, $m\ddot{x}$ and by substituting each angular velocity into pendulum's velocity, the following equations will be obtained as follows,

$$\begin{aligned} &\left(J_P + J_{G1} + J_{G2}N_1^2 + \left[J_{G3} + J_{eq}\right]N_2^2\right)\ddot{\theta} + N^2N_2^2C_{Te}\dot{\theta} + mgL\sin\theta = FL\cos\theta, \ \ \theta \geq 0 \\ &\left(J_P + J_{G1}N_3^2 + J_{G2} + \left[J_{G3} + J_{eq}\right]N_4^2\right)\ddot{\theta} + N^2N_4^2C_{Te}\dot{\theta} + mgL\sin\theta = FL\cos\theta, \ \ \theta < 0 \end{aligned} \tag{7}$$

where, $N = r_c/r_s$; $N_1 = r_{G1}/r_{G2}$; $N_2 = r_{G1}/r_{G3}$; $N_3 = r_{G2}/r_{G1}$; $N_4 = r_{G2}/r_{G3}$; and $C_{Te} = k_t k_m/(R_{in} + R_{LOAD})$.

Eq. (7) is such a nonlinear equation. By considering the small movement in the pendulum motion, here the linear approximation of small angle can be used for $sin\ \theta \approx \theta$ and $cos\ \theta \approx 1$. In addition, the above equation can be reformed to obtain F_{ext} as follows,

$$F_{ext} = \frac{1}{L}\begin{cases}\left(J_P + J_{G1}N_3^2 + J_{G2} + \left[J_{G3} + J_{eq}\right]N_4^2\right)\ddot{\theta} + N^2N_4^2C_{Te}\dot{\theta} + mgL\theta, & \theta < 0\\ \left(J_P + J_{G1} + J_{G2}N_1^2 + \left[J_{G3} + J_{eq}\right]N_2^2\right)\ddot{\theta} + N^2N_2^2C_{Te}\dot{\theta} + mgL\theta, & \theta \geq 0\end{cases} \quad (8)$$

where, F in Eq. (8) designates as damping force.

Parameters. Several parameters presented in this paper are taken by direct measurement, calculation and approximation. The moment of inertia in a gear is obtained by measuring its weight and considering the gear as a hollow disc. Moreover, the generator characteristics such as the current constant (α) and the voltage constant (β) are determined by direct measurements in each rotation per minute. Then the results are graphed and linearized to obtain parameter constants. To sum up, the parameters used for simulation are listed in Table 1.

Table 1. Parameters of the RPVA and the energy regeneration units

Parameter (unit)	Value	Parameter (unit)	Value	Parameter (unit)	Value
J_{G1} (kg.m^2)	2.2834x10^{-5}	N	9	g (m/s^2)	9.81
J_{G2} (kg.m^2)	2.2834x10^{-5}	N_1	1	β (A/rpm)	0.004359
J_{G3} (kg.m^2)	6.2279x10^{-7}	N_2	2	α_1 (V/rpm)	0.174
J_c (kg.m^2)	5.7180x10^{-6}	N_3	1	α_2 (V/rpm)	0.0033
J_{pl} (kg.m^2)	1.6073x10^{-7}	N_4	2	C_{Te} (T/rpm)	9.16x10^{-4}
J_s (kg.m^2)	1.2778x10^{-7}	m (kg)	10		
J_P (kg.m^2)	0.625	L (m)	0.25		

Results and Discussion

To conduct a numerical simulation, the input parameters must be known first. Therefore, the sinusoidal signal is used as an input and its equations can be given as follows,

$$\begin{aligned} x(t) &= A\sin 2\pi ft \\ \dot{x}(t) &= 2\pi fA\cos 2\pi ft \\ \ddot{x}(t) &= -(2\pi f)^2 A\sin 2\pi ft \end{aligned} \quad (9)$$

where, x, $\dot{x}$ and $\ddot{x}$ are the displacement, the velocity and the acceleration of the cart respectively, and also refer to Eq. (3), Eq. (7) and Eq. (8). A and f are the amplitude and the frequency of the sinusoidal signal, respectively.

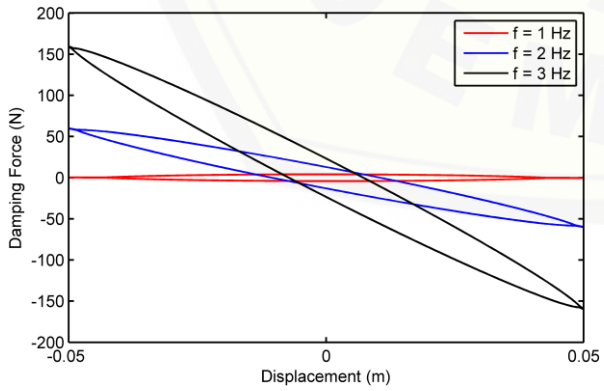

Fig. 5 Force-displacement characteristics with different frequencies

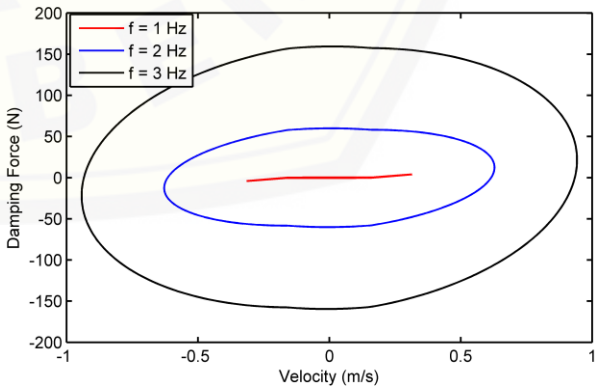

Fig. 6 Force-velocity characteristics with different frequencies

By simulating the above mathematical models into numerical simulation software, the damping force can be characterized. Fig. 5 and Fig. 6 show the force-displacement and force-velocity curve with fixed amplitude at 0.05 m and three different frequencies. When the frequency is set at 1 Hz, both force-displacement and force-velocity show more obviously relevant to basic damper [11]. As

increasing frequency, the curves become more likely relevant to the hysteretic damping but in opposite direction [12]. It can be caused by the multiplication result of the moment of inertia and the angular acceleration, in which the angular acceleration has a negative sign as described in Eq. (9).

Force-displacement and force-velocity is also evaluated with fixed frequency at 1 Hz and three different amplitudes, as shown in Fig. 7 and Fig. 8. Increasing amplitude does not make significance changes in the loop shape, compared with increasing frequency. From Fig. 8, there is constantly small force at low velocity that looks like a dead zone. This characteristic also refers to the multiplication result of the moment of inertia and the angular acceleration, in which the angular acceleration reaches the peak when the angular velocity around zero as described in Eq. (9).

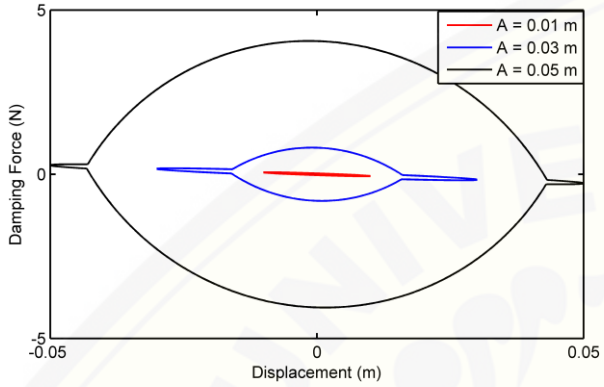

Fig. 7 Force-displacement characteristics with different amplitudes

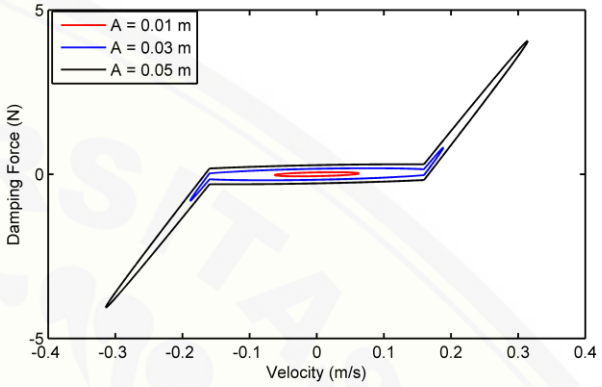

Fig. 8 Force-velocity characteristics with different amplitudes

The influences of the amplitude and the frequency as inputs can be obtained using 3D plot. Hence the results are depicted in Fig. 9, where X-axis defines the frequency that lies from 0.25 Hz to 5 Hz and Y-axis defines the amplitude that runs from 0.005 m to 0.05 m. It is obtained that force generated by the pendulum increases as long as the frequency and the amplitude arise.

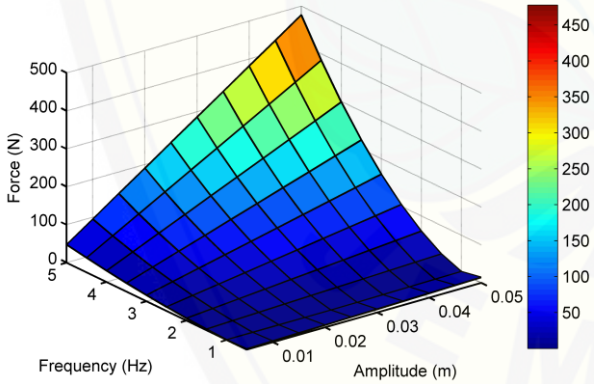

Fig. 9 The relation between frequencies and amplitudes to the damping force

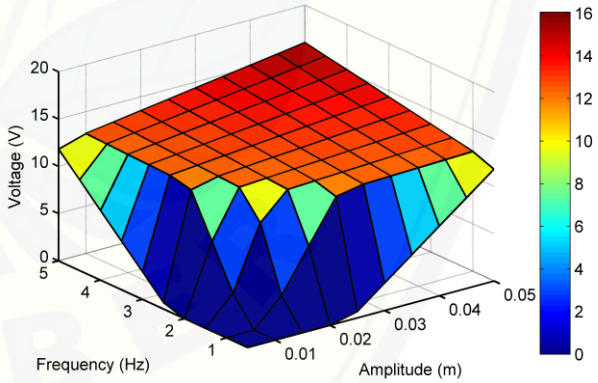

Fig. 10 The relation between frequencies and amplitudes to the voltage generated

The energy regeneration characteristics including the voltage, the current and the power generation will be evaluated using different amplitudes and frequencies. The voltage generated generally has the values that lie around 12V to 16.5V, as shown in Fig. 10. It means that the charging process on the battery works. Deliberately, the voltage is limited at 16.5V to prevent any damages on the battery. To obtain the voltage characteristic, here the plot of voltage-velocity is depicted in Fig. 11 with the amplitude and the frequency fixed at 0.05 m and 5 Hz, respectively.

From Fig. 11, there is dead zone at low velocities in which the generator cannot produce electricity. Then the voltage increases significantly until the angular velocity reaches 0.74 rad/s. It causes by the minimum requirement of DC step up to boost up the voltage. When the generator produces at least 3V, the DC step up suddenly boosts up the voltage to 12 V. This phenomenon can be related to Fig. 10 where the sinusoidal inputs are set up at low frequencies and amplitudes.

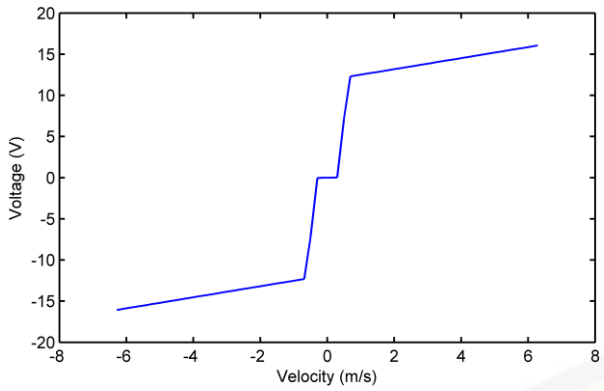

Fig. 11 Voltage-velocity characteristics

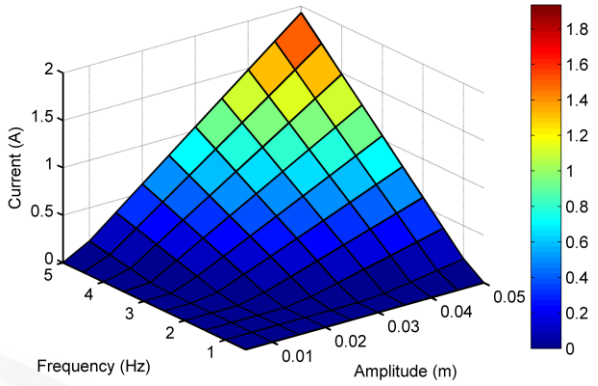

Fig. 12 The relation between frequencies and amplitudes to the current generated

The influences between frequencies and amplitudes to the current and the power generated are depicted in Fig. 12 and Fig. 13, respectively. They show the same trend line, in which there is no current at low frequencies and low amplitudes. It can be related to the voltage characteristic at low level, where there is no sufficient voltage to charge the battery. To sum up, the negative sign in the voltage, the current and the power generated mean that the pendulum works in CW direction.

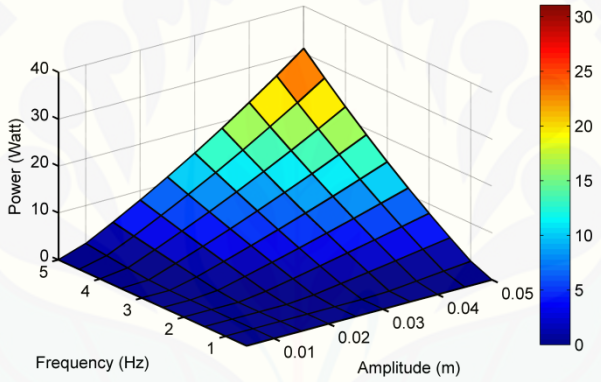

Fig. 13 The relation between frequencies and amplitudes to the power generated

Conclusion

The design of pendulum using motion rectifier as vibration absorber and energy harvester is proposed and analyzed. Its mathematical model is derived and studied under sinusoidal signal inputs. Generally, the damping force produced by systems fulfills hysteretic damper in opposite direction that caused by the moment of inertia in gears. Dead zone in the voltage, the current and the power generated is occurred at low velocities, in which the generator cannot produce sufficient electric.

This analysis only determines the characteristics of damping force and energy regeneration. The influences of hysteretic damper, caused by multiplication of the moment of inertia and the acceleration, must be analyzed to obtain the ability of its systems reducing vibrations.

Acknowledgement

This work was supported by Grant No: 10029/UN25/LT/2016 from the Research Institute of the University of Jember and the authors wish to thank for this support.

References

[1] X. Liu, An Electromagnetic Energy Harvesting for Powering Consumer Electronics. Master Thesis. Clemson University, South Carolina, 2012.

[2] W. Ding, B. Song, Z. Mao, K. Wang, Experimental Investigations on a Low Frequency Horizontal Pendulum Ocean Kinetic Energy Harvester for Underwater Mooring Platforms, J. Mar. Sci. Technol. 21 (2016) 359-367.

[3] I. Iliuk, J.M. Balthazar, A.M. Tusset, J.R.C. Piqueira, B. Rodigues de Pontez, J.L.P. Felix, A.M. Bueno, A Non-Ideal Portal Frame Energy Harvester Controlled Using a Pendulum, Eur. Phys. J. Spec. Top. 222 (2013) 1575-1586.

[4] K. Kęcik, Energy Harvesting of a Pendulum Vibration Absorber, Przegląd Elektrotechniczny. 07 (2013) 169-172.

[5] P.V. Malaji, S.F. Ali, Analysis of Energy Harvesting from Multiple Pendulums with and without Mechanical Coupling, Eur. Phys. J. Spec. Top. 224 (2015) 2823-2838.

[6] M. Wiercigroch, A. Najdecka, V. Vaziri, Nonlinear Dynamics of Pendulums System for Energy Harvesting, Vibration Problems ICOVP 2011. (2011) 35-42.

[7] C. Cepnik, R. Lausecker, U. Wallrabe, Review on Electromagnetic Energy Harvester-A Classification Approach, Micromachines. 4 (2013) 168-196.

[8] S.N.H. Syuhri, The Influences of Changing Mechanical and Electrical Damping for Total Damping Force and Energy Regeneration on Hydraulic Regenerative Suspension. Master Thesis. Institute Technology of Sepuluh Nopember, Surabaya, 2015. (in Indonesian)

[9] Z. Li, L. Zuo, G. Luhrs, L. Lin, Y. Qin, Electromagnetic Energy-Harvesting Shock Absorbers: Design, Modeling, and Road Tests, IEEE Trans. Veh. Technol. 62 (2013) 1065-1074.

[10] Z. Li, L. Zuo, J. Kuang, G. Luhrs, Energy-Harvesting Shock Absorber with a Mechanical Motion Rectifier, Smart Mater. Struct. 22 (2013).

[11] J.C. Dixon, The Shock Absorber Handbook, second ed., John Wiley & Sons, Ltd, 2007.

[12] S.S. Rao, Mechanical Vibrations, fifth ed., Pearson, New Jersey, 2011.